

# Supplementary Materials for: Observation of flat-band and band transition in the synthetic space

Guangzhen Li<sup>a,†</sup>, Luoja Wang<sup>a,†</sup>, Rui Ye<sup>a</sup>, Shijie Liu<sup>a</sup>, Yuanlin Zheng<sup>a,b</sup>, Luqi Yuan<sup>a,\*</sup>,  
Xianfeng Chen<sup>a,b,c,\*</sup>

<sup>a</sup>State Key Laboratory of Advanced Optical Communication Systems and Networks, School of Physics and Astronomy, Shanghai Jiao Tong University, Shanghai 200240, China

<sup>b</sup>Shanghai Research Center for Quantum Sciences, Shanghai 201315, China

<sup>c</sup>Collaborative Innovation Center of Light Manipulation and Applications, Shandong Normal University, Jinan 250358, China

**Keywords:** synthetic dimensions, ring resonators, dynamic modulation, flat band.

\*Luqi Yuan, [yuanluqi@sjtu.edu.cn](mailto:yuanluqi@sjtu.edu.cn); Xianfeng Chen, [xfchen@sjtu.edu.cn](mailto:xfchen@sjtu.edu.cn)

†Guangzhen Li, Luoja Wang. These authors contribute equally to this work.

## 1 Theory of the band structure measurement in two rings

Here, we provide the detailed derivations of the transmission spectra recorded from the drop-port output of the specific excited ring, which are then used to obtain the time-resolved band structures for the two cases  $A \text{ in} \rightarrow A \text{ out}$  and  $B \text{ in} \rightarrow B \text{ out}$ .

Following the treatment in Refs. 24-25, we start with considering the Hamiltonian in Eq. (1) in the main text. One can get the coupled amplitude equations for  $A \text{ in} \rightarrow A \text{ out}$  in the interaction picture by taking the rotating-wave approximation (RWA), which results in

$$\begin{aligned}
 \dot{\tilde{v}}_{a,n} &= (i\Delta\omega - \gamma)\tilde{v}_{a,n} - i\kappa\tilde{v}_{b,n} - ig(\tilde{v}_{c,n}e^{i\phi} + \tilde{v}_{c,n-1}e^{-i\phi}) + i\sqrt{\gamma_A}S_{\text{in}}^A e^{i(n-n_0/2)\Omega t}, \\
 \dot{\tilde{v}}_{b,n} &= (i\Delta\omega - \gamma)\tilde{v}_{b,n} - i\kappa\tilde{v}_{a,n}, \\
 \dot{\tilde{v}}_{c,n} &= (i\Delta\omega - \gamma)\tilde{v}_{c,n} - ig(\tilde{v}_{a,n}e^{-i\phi} + \tilde{v}_{a,n+1}e^{i\phi}) + i\sqrt{\gamma_A}S_{\text{in}}^A e^{i(n+1/2-n_0/2)\Omega t}, \\
 S_{\text{out}}^A &= -i\sqrt{\gamma_A}e^{-i\Delta\omega t} \sum_n (\tilde{v}_{a,n}e^{-i\omega_n t} + \tilde{v}_{c,n}e^{-i\omega_n t - i\Omega t/2}),
 \end{aligned} \tag{S1}$$

where  $\tilde{v}_{a,n}$ ,  $\tilde{v}_{b,n}$ , and  $\tilde{v}_{c,n}$  are the amplitudes of the photon states of the frequency modes  $A_n$ ,  $B_n$ , and  $C_n$ .  $S_{\text{in}}^A$  is the envelope of the laser source through the input port of ring A with an input frequency  $\omega = \omega_0 + n_0\Omega/2 + \Delta\omega$ . Here, we define  $n_0$  to distinguish the modes  $A_n$  and  $C_n$ , where  $n_0 = 0$  and  $n_0 = 1$  refer to the situations of the input field near the reference frequencies  $\omega_0$  and  $\omega_0 + \Omega/2$ , corresponding to modes  $A_n$  and  $C_n$  separated by  $\Omega/2$  along the frequency dimension,

respectively. We then transform the amplitudes of the modes into the  $k_f$  space by defining

$$\psi_{k_f}^A = \sum_n \tilde{v}_{a,n} e^{-in\Omega k}, \quad \psi_{k_f}^B = \sum_n \tilde{v}_{b,n} e^{-in\Omega k}, \quad \psi_{k_f}^C = \sum_n \tilde{v}_{c,n} e^{-i(n+1/2)\Omega k}, \quad (\text{S2})$$

which gives

$$\begin{aligned} \dot{\psi}_{k_f}^A &= (i\Delta\omega - \gamma)\psi_{k_f}^A - i2g \cos(\Omega k_f/2 + \phi)\psi_{k_f}^C - i\kappa\psi_{k_f}^B + i\sqrt{\gamma_A} S_{\text{in}}^A e^{-in_0\Omega t/2} \sum_n e^{-in\Omega(k_f-t)}, \\ \dot{\psi}_{k_f}^B &= (i\Delta\omega - \gamma)\psi_{k_f}^B - i\kappa\psi_{k_f}^A, \\ \dot{\psi}_{k_f}^C &= (i\Delta\omega - \gamma)\psi_{k_f}^C - i2g \cos(\Omega k_f/2 + \phi)\psi_{k_f}^A + i\sqrt{\gamma_A} S_{\text{in}}^A e^{-in_0\Omega t/2} \sum_n e^{-i(n+1/2)\Omega(k_f-t)}, \end{aligned} \quad (\text{S3})$$

and the amplitude of the output field becomes

$$S_{\text{out}}^A = -i\sqrt{\gamma_A} e^{-i\omega_0 t - i\Delta\omega t} \left[ \psi_{k_f}^A(t) + \psi_{k_f}^C(t) \right] \Big|_{k_f=t}. \quad (\text{S4})$$

By using the definition of column vectors  $|\psi_{k_f}\rangle = (\psi_{k_f}^A, \psi_{k_f}^B, \psi_{k_f}^C)^T$  and  $|S_{\text{in}}^A\rangle = (1, 0, e^{-i\Omega(k_f-t)/2})^T$ , we can rewrite Eq. (S3) into a compact form as

$$[\Delta\omega + i\gamma - (H_{k_f} - i\partial_t)] |\psi_{k_f}\rangle + \sqrt{\gamma_A} \sum_n e^{-in\Omega(k_f-t)} e^{-in_0\Omega t/2} |S_{\text{in}}^A\rangle = 0, \quad (\text{S5})$$

where  $H_{k_f}$  is the Hamiltonian in  $k_f$  space given by Eq. (3). The corresponding eigenvalues and eigenstates satisfy  $H_{k_f}\psi_{k_f,j} = \varepsilon_{k_f,j}\psi_{k_f,j}$  for the case of RWA, which are shown in Eqs. (4)-(5).

For a more general case of modulation without using the RWA,  $H_{k_f}$  is time-dependent with the period of  $T = 4\pi/\Omega$ . At steady state, the eigenstates of  $H_{k_f}$  form a complete basis for expanding  $\psi_{k_f}(t)$ . By taking the inner product of Eq. (S5) with  $\langle\psi_{k_f,j}|$ , defined as  $\langle f(t)|g(t)\rangle_T = (1/T) \int_0^T dt f^*(t) \cdot g(t)$ , we obtain the expansion coefficients of the output field in terms of the

eigenstates as

$$\begin{aligned}
& \langle \psi_{k_f, j} | \psi_{k_f} \rangle_T \\
&= \frac{-\sqrt{\gamma_A} S_{\text{in}}^A}{\Delta\omega + i\gamma - \varepsilon_{k_f, j}} \frac{1}{T} \int_0^{\frac{4\pi}{\Omega}} dt \sum_n e^{-in\Omega(k_f - t)} e^{-in_0\Omega t/2} \left[ \psi_{k_f, j}^{A*}(t) + e^{-i\Omega(k_f - t)/2} \psi_{k_f, j}^{C*}(t) \right] \\
&= \frac{-\sqrt{\gamma_A} S_{\text{in}}^A}{\Delta\omega + i\gamma - \varepsilon_{k_f, j}} \frac{1}{T} \int_0^{\frac{4\pi}{\Omega}} dt \left\{ \frac{T}{2} \left[ \delta(k_f - t) + \delta\left(k_f + \frac{2\pi}{\Omega} - t\right) + \delta\left(k_f - \frac{2\pi}{\Omega} - t\right) \right] \right. \\
&\quad \left. e^{-in_0\Omega t/2} \left[ \psi_{k_f, j}^{A*}(t) + e^{-i\Omega(k_f - t)/2} \psi_{k_f, j}^{C*}(t) \right] \right\} \\
&= \frac{-\sqrt{\gamma_A} S_{\text{in}}^A}{\Delta\omega + i\gamma - \varepsilon_{k_f, j}} \frac{1}{2} \left[ e^{-in_0\Omega k_f/2} \left( \psi_{k_f, j}^{A*} + \psi_{k_f, j}^{C*} \right) + e^{-in_0\Omega k_f/2 + in_0\pi} \left( \psi_{k_f, j}^{A*} - \psi_{k_f, j}^{C*} \right) \right].
\end{aligned} \tag{S6}$$

If  $n_0 = 0$ , one can get the output field form the drop-port of ring A

$$S_{\text{out}}^A = i\gamma_A S_{\text{in}}^A e^{-i\omega t} \sum_j \left. \frac{(\psi_{k_f, j}^A + \psi_{k_f, j}^C) \psi_{k_f, j}^{A*}}{\Delta\omega + i\gamma - \varepsilon_{k_f, j}} \right|_{k_f=t}. \tag{S7}$$

On the other hand, one can also have the output field for  $n_0 = 1$ , which is

$$S_{\text{out}}^A = i\gamma_A S_{\text{in}}^A e^{-i\omega t} \sum_j \left. \frac{(\psi_{k_f, j}^A + \psi_{k_f, j}^C) \psi_{k_f, j}^{C*}}{\Delta\omega + i\gamma - \varepsilon_{k_f, j}} \right|_{k_f=t}. \tag{S8}$$

Equation (S7)-(S8) indicate that the output amplitude at time  $t$  is exclusively determined by the eigenvalues and eigenstates from the band structure of the synthetic one-dimensional Lieb lattice. Under the conditions of  $\gamma \ll \Omega/2$  and  $g < \Omega/4$ , only the term closest to the input frequency  $\omega$  contributes significantly to the sum. Then the normalized time-resolved transmissions can be approximately given by

$$\begin{aligned}
T_{\text{out}}^A(t = k_f; \Delta\omega) &= \frac{\gamma_A^2 |\psi_{k_f, j}^A|^2 |\psi_{k_f, j}^A + \psi_{k_f, j}^C|^2}{(\Delta\omega - \varepsilon_{k_f, j})^2 + \gamma^2}, \\
T_{\text{out}}^A(t = k_f; \Delta\omega + \Omega/2) &= \frac{\gamma_A^2 |\psi_{k_f, j}^C|^2 |\psi_{k_f, j}^A + \psi_{k_f, j}^C|^2}{(\Delta\omega - \varepsilon_{k_f, j})^2 + \gamma^2}.
\end{aligned} \tag{S9}$$

Similarly, for the case of B *in*  $\rightarrow$  B *out*, one can obtain the input/output coupled amplitude

equations as

$$\begin{aligned}
\dot{\tilde{v}}_{a,n} &= (i\Delta\omega - \gamma)\tilde{v}_{a,n} - i\kappa\tilde{v}_{b,n} - ig(\tilde{v}_{c,n}e^{i\phi} + \tilde{v}_{c,n-1}e^{-i\phi}), \\
\dot{\tilde{v}}_{b,n} &= (i\Delta\omega - \gamma)\tilde{v}_{b,n} - i\kappa\tilde{v}_{a,n} + i\sqrt{\gamma_B}S_{\text{in}}^B e^{i(n-n_0/2)\Omega t}, \\
\dot{\tilde{v}}_{c,n} &= (i\Delta\omega - \gamma)\tilde{v}_{c,n} - ig(\tilde{v}_{a,n}e^{-i\phi} + \tilde{v}_{a,n+1}e^{i\phi}), \\
S_{\text{out}}^B &= -i\sqrt{\gamma_B}e^{-i\Delta\omega t} \sum_n \tilde{v}_{b,n}e^{-i\omega_n t}.
\end{aligned} \tag{S10}$$

Further, we convert Eq. (S10) into the  $k_f$  space

$$\begin{aligned}
\dot{\psi}_{k_f}^A &= (i\Delta\omega - \gamma)\psi_{k_f}^A - i2g \cos(\Omega k_f/2 + \phi)\psi_{k_f}^C - i\kappa\psi_{k_f}^B, \\
\dot{\psi}_{k_f}^B &= (i\Delta\omega - \gamma)\psi_{k_f}^B - i\kappa\psi_{k_f}^A + i\sqrt{\gamma_B}S_{\text{in}}^B e^{-in_0\Omega t/2} \sum_n e^{-in\Omega(k_f-t)}, \\
\dot{\psi}_{k_f}^C &= (i\Delta\omega - \gamma)\psi_{k_f}^C - i2g \cos(\Omega k_f/2 + \phi)\psi_{k_f}^A, \\
S_{\text{out}}^B &= -i\sqrt{\gamma_B}e^{-i\omega_0 t - i\Delta\omega t} \psi_{k_f}^B(t) \Big|_{k_f=t}.
\end{aligned} \tag{S11}$$

Using the column vector of  $|S_{\text{in}}^B\rangle = (0, 1, 0)^T$ , the input/output equations in Eq. (S11) become

$$[\Delta\omega + i\gamma - (H_{k_f} - i\partial_t)] |\psi_{k_f}\rangle + \sqrt{\gamma_B} \sum_n e^{-in\Omega(k_f-t)} e^{-in_0\Omega t/2} |S_{\text{in}}^B\rangle = 0. \tag{S12}$$

Then one gets the steady-state output field from the drop port of ring B

$$S_{\text{out}}^B = i\gamma_B S_{\text{in}}^B e^{-i\omega t} \sum_j \frac{\psi_{k_f,j}^B \psi_{k_f,j}^{B*} (1 + e^{in_0\pi})/2}{\Delta\omega + i\gamma - \varepsilon_{k_f,j}} \Big|_{k_f=t}, \tag{S13}$$

and the normalized drop-port transmission for  $n_0 = 0$  is

$$T_{\text{out}}^B(t = k_f; \Delta\omega) = \frac{\gamma_B^2 |\psi_{k_f,j}^B|^4}{(\Delta\omega - \varepsilon_{k_f,j})^2 + \gamma^2}. \tag{S14}$$

Therefore, We obtain the drop-port transmissions for the two cases, where Eq. (S9) and Eq. (S14) are Eqs. (7)-(8) and Eq. (6) in the main text, respectively.

## 2 Experimental setup

The frequency of the laser source can be finely tuned over 30 GHz by applying an external ramp signal to its frequency modulation input, with the central wavelength located at 1550.92 nm. Near 50% of the laser source is sent to an acousto-optic modulation (AOM) for frequency shift and heterodyne beating with the drop-port output. In each ring, a  $2 \times 2$  fiber coupler couples 1% of the remaining 50% laser source to the ring resonator, after which a polarization controller is used to adjust the polarization of laser circulating in the ring. To achieve a high quality factor for the resonator, a semiconductor optical amplifier (SOA) is used to compensate the loss in the ring with a maximum gain of 10 dB. A dense wavelength division multiplexing with a central wavelength of 1550.92 nm (international telecommunication union channel 33) is used to filter the amplified emission noise from SOA. Ring A undergoes dynamic modulation by a lithium niobate EOM with a 10 GHz bandwidth, which is driven by an arbitrary waveform generator with 200 MHz bandwidth. A  $1 \times 2$  fiber coupler couples 0.5% of the signal out of the ring, which is then amplified by an erbium-doped optical fiber amplifier (with maximum gain of 12 dB) to boost the signal-to-noise ratio before it gets detected by a fast InGaAs photodiode (850 to 1650 nm with 10 GHz bandwidth) and sent to the oscilloscope (5 Gsamples/s with 1 GHz bandwidth). For the flat band structure measurement (Fig. 3 and Fig. 4 in the main text), we disconnect the AOM path, and only connect it for the resonant mode observation (Fig. 5 in the main text). In addition, we also place an EOM in ring B just for calibrating the length of ring B, which is not shown in Fig. S1.

The lengths of the two rings need accurate calibration for stabilizing the connectivity between the resonant modes to construct the synthetic Lieb lattice. We first separately measure the FSRs of ring A and ring B by disconnecting the 70:30 fiber coupler. For each ring, we vary the modulation frequency by linearly sweeping the input frequency until the modulation sidebands fully overlap with the resonant modes. We then adjust fiber's length to make up for the required FSR difference. One can also place an optical delay in the ring to finely tuning the length. Noting that the fiber coupler used to couple the two rings together in Fig. S1 keeps 70% of the light power remained in the excited ring and the left 30% coupled to the other ring no matter which ring we choose to excite, which gives the same coupling strengths for both cases.

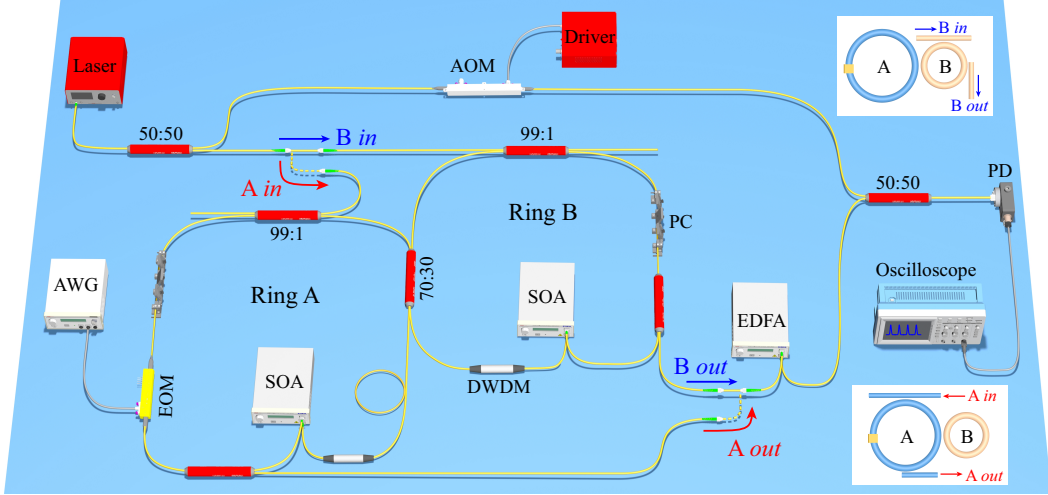


**Fig S1** Experimental setup. EOM: electro-optic phase modulator. AOM: acousto-optic modulation. SOA: semiconductor optical amplifier. AWG: arbitrary waveform generator. EDFA: erbium-doped optical fiber amplifier. PC: polarization controller. DWDM: dense wavelength division multiplexing. PD: photodiode. Inserted: sketches of  $B\ in \rightarrow B\ out$  and  $A\ in \rightarrow A\ out$ .

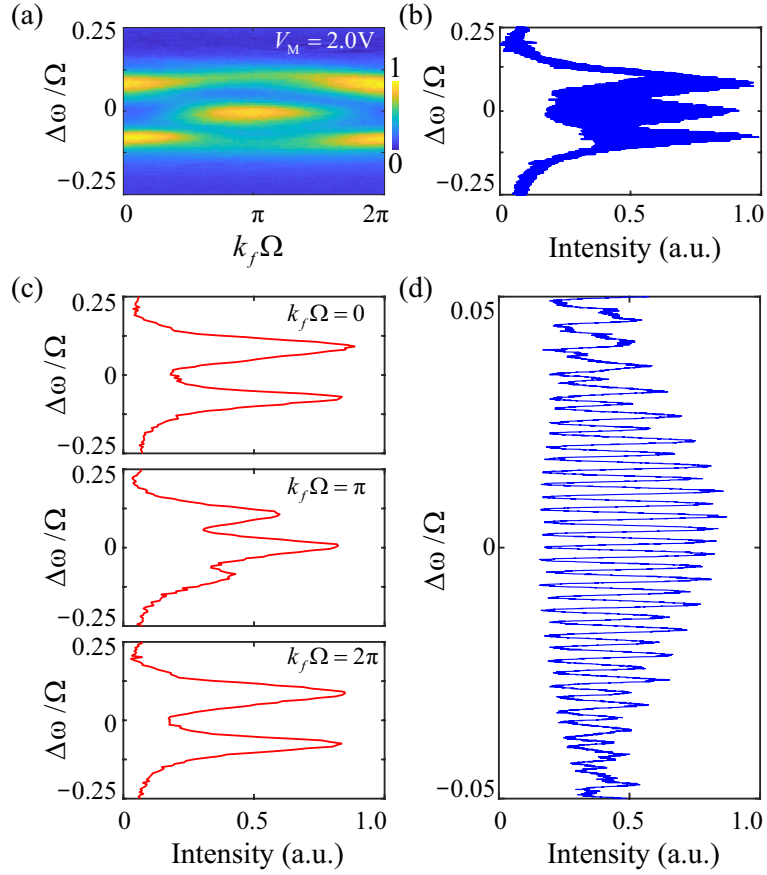


**Fig S2** (a) Experimentally measured band structure and (b) transmission spectrum of Fig. 2(c1) and 2(c3) in the main text. (c) Vertical slices of the band structure in (a) at times  $0$ ,  $\pi$ , and  $2\pi$ , respectively. (d) Enlarged transmission spectrum of (b).

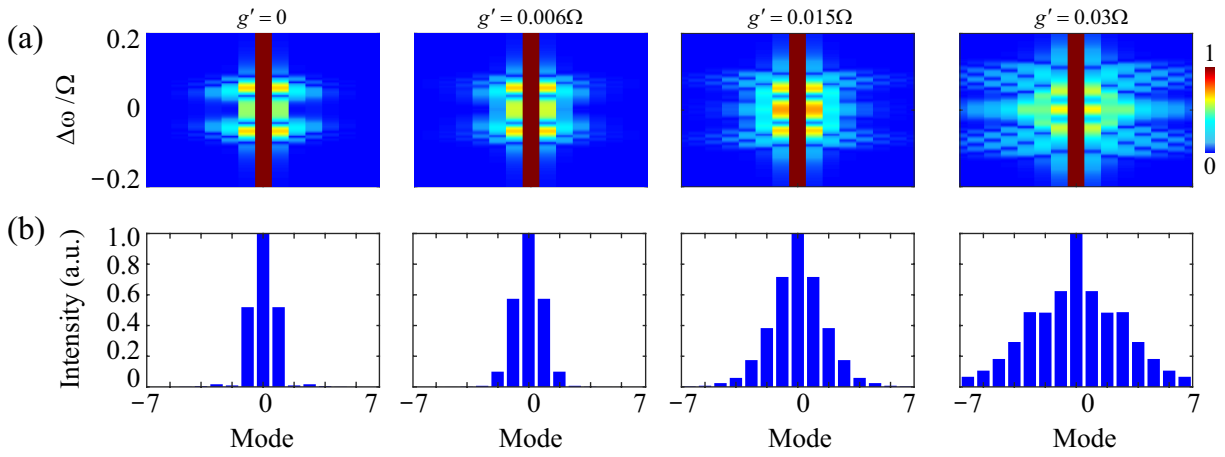


**Fig S3** (a) Simulated mode spectra by adding long-range couplings for the case of B *in*→B *out* with varied coupling strength  $g'$ , where  $g = \kappa = 0.06\Omega$  and  $\gamma = 0.03\Omega$ . (b) The corresponding mode distributions of (a) with input frequency detuning located at the flat band ( $\Delta\omega = 0$ ).